IEEE Access
Multidisciplinary ⋮ Rapid Review ⋮ Open Access Journal

Received August 27, 2021, accepted September 16, 2021, date of publication September 20, 2021,
date of current version September 28, 2021.

Digital Object Identifier 10.1109/ACCESS.2021.3114301

A Method for Fans' Potential Malfunction Detection of ONAF Transformer Using Top-Oil Temperature Monitoring

LUJIA WANG[1,2], (Member, IEEE), WANWAN ZUO[1], ZHI-XIN YANG[2], (Member, IEEE), JIANWEN ZHANG[1], AND ZHENLU CAI[1]

[1]School of Electrical and Power Engineering, China University of Mining and Technology, Xuzhou 221116, China
[2]State Key Laboratory of Internet of Things for Smart City and Department of Electromechanical Engineering, University of Macau, Macau SAR, China

Corresponding author: Zhi-Xin Yang (zxyang@um.edu.cn)

This work was supported in part by the Fundamental Research Funds for the Central Universities under Grant 2021QN1064; in part by the Science and Technology Development Fund, Macau, under Grant 0018/2019/AKP, Grant 0008/2019/AGJ, and Grant SKL-IOTSC-2021-2023; in part by the Ministry of Science and Technology of China under Grant 2019YFB1600700; in part by Zhuhai-Hong Kong-Macau Collaboration Fund under Grant ZH22017002200001PWC; and in part by the University of Macau under Grant MYRG2018-00248-FST and Grant MYRG2019-0137-FST.

ABSTRACT The fan is one of the key components of the power transformer cooling system. The operating condition of fans determines transformers' internal temperature rise and long-term reliability. However, at present, the fans' condition monitoring only includes switch status (online) and regular maintenance (offline), online direct monitoring of the fans' operating condition is lacking due to economic costs. In view of the above-mentioned problem, this paper proposes a transformer fan early fault detection method based on the oil exponent, which is monitored by the existing transformer top-oil temperature data, thereby detecting the abnormality of the fans. In this method, the oil exponent was chosen as the characteristic criterion. First, to obtain the range of oil exponent in different cooling modes, a set of physical models describing global oil flow and its interaction with air was established based on fluid dynamics and heat transfer principle. Then, regarding the constantly changing top-oil temperature, ambient temperature and load current, an oil exponent tracking algorithm using particle swarm optimization (PSO) was proposed within an improved IEC dynamic thermal model. The operation data from an oil-immersed transformer with a rated capacity of 120-MVA and rated voltage of 220-kV was selected to verify the above methods under two different scenarios.

INDEX TERMS Power transformer, cooling system, fan, top-oil temperature, condition monitoring, oil exponent.

I. INTRODUCTION

As the key equipment for power delivery, the transformers' safety and stability is significant to the power system reliability [1], [2]. Meanwhile, as a large-scale implementation of photovoltaic panels, wind farms and electric vehicles etc., transformers get overloaded inevitably in a local area or within a short period, which further makes the winding hot-spot temperature face the potential risk of exceeding the limit [3]. To ensure that the transformer temperature rise is within a reasonable limit, it is vital to keep the normal operation of the transformer cooling system.

The associate editor coordinating the review of this manuscript and approving it for publication was Mauro Tucci.

Oil pumps and fans are only two active parts of cooling system for oil-immersed transformers. For oil-forced (OF) or oil-directed (OD) transformers, they have a lower fault tolerance due to the existence of pumps, so nowadays utilities tend to use more oil-natural (ON) transformers even at higher voltage levels. On the other hand, for many ON transformers, the external fans become the only active part to enhance the heat dissipation efficiency, *i.e.*, turning to oil-natural air-forced (ONAF) cooling mode. Therefore, external fans for radiator are key factor to affect the temperature rise of oil-immersed transformers [4].

Several attempts have been made to design, structure optimization and performance enhancement for radiator with fans. For the design of radiator with fans, a series of numerical

simulation has been validated to find the optimal size and structure of the heat sink [5]. A forced air-cooling system for motors was designed using lumped-parameter thermal models, which greatly reduces the temperature rise of windings and magnets [6]. In addition, Zhao *et al.* [7] has discussed the effect of heat conduction of radiator wall on the overall heat dissipation. For the structure optimization of radiator with fans, Dasgupta *et al.* [8] has proved that adding chimneys or enclosures around the radiator can enhance the air flow performance. To improve the efficiency of calculation, a complete thermo-hydraulic radiator model was proposed which combined the fan characteristics and the radiator geometry [9]. For the cooling performance enhancement of radiator with fans, CFD simulations and corresponding experiments have showed that the horizontal blowing of the offset cooling fan can achieve the best cooling efficiency [10]. Besides, Kim *et al.* [11] also found a best fan combination though changing the relative position of two perpendicular blowing directions.

The fan is a typical type of rotating machine, and some large-scale fans such as wind turbines have been well monitored online and offline. Many researchers have established a variety of methods for condition monitoring and fault diagnosis methods of rotating machine based on current signal, vibration signal and so on [12]–[14]. However, for the fans of the cooling system within the power transformer, it has a pretty lower power for a single unit and always is used as a piece of auxiliary equipment for the transformer, so it has not been specially monitored.

In most practice scenarios, the only online monitoring information is the switch status of the fans of the cooling system within the power transformer, *i.e.*, the utilities just know the numbers of operating fans. Besides, the condition detection method for the fans is mainly regular maintenance, which cannot achieve the real-time monitoring and is difficult to find the potential failures. For a large number of transformers, it is not economical to pre-install or re-equip more sensors (like current, vibration as we described above) to fulfill better condition awareness. So, it is sensible to find a "kill two birds with one stone" way from the existing monitoring.

The top-oil temperature (TOT) has always been monitored by direct measurement for power transformer [15], [16]. Therefore, it is better to fully use TOT monitoring. The key is to establish the link between the condition of fans and the information implied within TOT dynamics. Many researchers have explored the TOT modelling to achieve a better accuracy [17]. On one hand, different model frameworks were proposed to predict or cover the TOT variation [18], [19]. On the other hand, if the modelling framework is determined, it is critical to find a group of accurate thermal parameters [20]–[22]. The authors also used to research the TOT modelling, especially investigating one dominant thermal parameter: oil exponent, which contains much information [23]. So, in the manuscript, the first attempt is to find the connection between fans' condition (mainly air flow rate) and oil exponent.

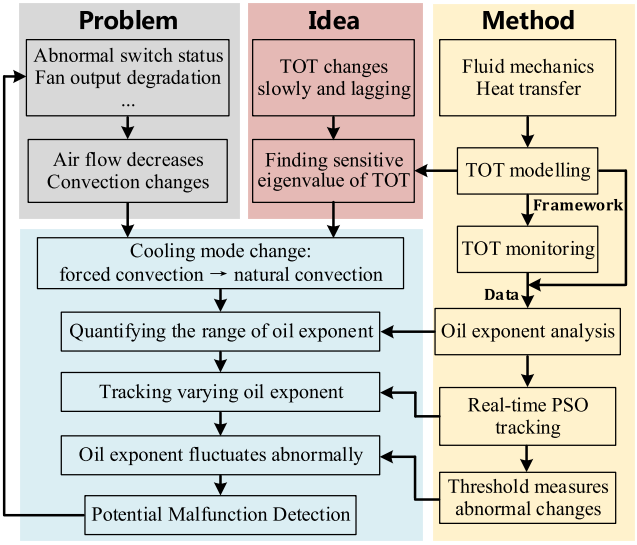

FIGURE 1. The flowchart of proposed method for detecting abnormal air flow from fans.

In this paper, in order to detect fans' gradual malfunction without installing more sensors, a method using the existing TOT monitoring was proposed. In this method, oil exponent was selected to indicate the condition of fans. First, for two extreme cases, *i.e.*, operation in ONAF cooling mode at full power and oil-natural air-natural (ONAN) cooling mode, the oil exponent was modelled and analyzed. Secondly, the oil exponent is solved and compared based on the calculation results to measure the change of fan airflow. Finally, the oil exponent is monitored in real time using PSO based on the IEC empirical formula, which is in accordance with actual fans' condition.

II. BASIS AND ROUTE OF PROPOSED METHOD

The air volume distinguishes the cooling modes between natural convection and forced convection. The cooling mode directly affects the TOT of transformer. So, the key is to find an eigenvalue that can quantify the two cooling modes, that is, reflecting the change of air volume from fans. According to the definition of oil exponent, the calculation fitting of oil exponent directly involves the oil temperature of the transformer, and since the operation of the cooling fan has a direct effect on the oil temperature, from this logic, which is shown in the logical technical flowchart depicted in Figure 1, we want to use the oil exponent to link the fan operation status to the oil temperature for the direct purpose of potential cooling fan fault detection through monitoring of the top oil temperature. This led to the modeling of the top oil temperature calculation for the two fan operating states, with the aim of finding the difference in the oil exponent.

The results of oil exponent calculation and the study of the measured data show that for the same transformer, the change in the operating state of the fan from fully on to half on to fully off not only directly affects the trend of the oil temperature,

but also indirectly affects the specific reference value of the oil exponent. Since oil exponent has always been used in IEC dynamic thermal model, the framework of an improved IEC top-oil thermal model was selected to track the variation using the TOT monitoring.

III. OIL TEMPERATURE MODELLING IN DIFFERENT AIR-COOLING MODES

A. THERMAL-HYDRAULIC MODELLING IN ONAN MODE

1) CONSERVATION FOR OIL FLOW MOMENTUM AND ENERGY

Under ON cooling mode, the oil flow density inside transformer changes due to the oil temperature rise. The resulting thermal buoyancy lift (Δp_{d}) of the oil flow is balanced with the fluid resistance:

$$\Delta p_d = \rho_{\mathrm{oil}}(T) \cdot g \cdot \beta_{\mathrm{oil}} \cdot S \tag{1}$$

where $\rho_{\mathrm{oil}}(T)$ is the density fitting function of the oil, which is dependent on the oil temperature; g is the acceleration of gravity; β_{oil} is the coefficient of thermal expansion. S can be calculated as [24], [25]:

$$S = \left(\Delta y - \frac{y_{\mathrm{ra}}}{2}\right)(T_{\mathrm{oil2}} - T_{\mathrm{oil1}}) + y_{\mathrm{ra}}(T_{\mathrm{oil2}} - T_{\mathrm{amb}}) - y_{\mathrm{ra}}\frac{T_{\mathrm{oil2}} - T_{\mathrm{oil1}}}{\ln(T_{\mathrm{oil2}} - T_{\mathrm{amb}}) - \ln(T_{\mathrm{oil1}} - T_{\mathrm{amb}})} \tag{2}$$

where Δy is the height difference between the middle point of the radiator and that of the winding; y_{ra} is the radiator height; T_{oil2} is the top-oil temperature and T_{oil1} is the bottom-oil temperature; ambient air temperature T_{amb} means the air temperature far enough away from the radiator.

For the oil flow in the panel of radiator, the oil channel could be regarded as a rectangle with a width of a_{oil} and height of b_{oil}, so the oil flow (Q_{oil}) was calculated as:

$$Q_{\mathrm{oil}} = -\frac{d(\Delta p_{\mathrm{d}})}{d\left[S/(T_{\mathrm{oil2}} - T_{\mathrm{oil1}})\right]} \frac{1}{\rho_{\mathrm{oil}}(T) \cdot v_{\mathrm{oil}}(T)} \frac{32 \cdot s_{\mathrm{c}}^3}{\eta \cdot d_{\mathrm{c}}^2} \tag{3}$$

where $v_{\mathrm{oil}}(T)$ is the kinematic viscosity of the oil, s_{c} is the area of the oil channel, d_{c} is the perimeter of the channel, and η is a constant related to the shape of the channel.

The total loss P generated by winding and iron core is transferred to the oil in the form of heat. From the perspective of energy conservation, then:

$$P = \rho_{\mathrm{oil}}(T) \cdot c_{\mathrm{oil}}(T) \cdot Q_{\mathrm{oil}} \cdot (T_{\mathrm{oil2}} - T_{\mathrm{oil1}}) \tag{4}$$

where $c_{\mathrm{oil}}(T)$ is the specific heat capacity of the oil.

2) CONSERVATION FOR AIR FLOW MOMENTUM AND ENERGY

For the ONAN transformer, the air side is in a natural convection state, satisfying momentum conservation. It is considered that the thermal lift force of the air flow (Δp_{air}) and the friction force between the air and the fins are balanced, then:

$$\frac{2\tau_w}{a_{\mathrm{air}}} = \frac{1}{2}(\beta\rho\Delta T)_{\mathrm{air}}\, g \tag{5}$$

According to Dean's equivalent formula [26], the shear stress (τ_w) on the fins surface is:

$$\tau_w = 0.0365 \cdot \rho_{\mathrm{air}} \cdot V_{\mathrm{air}}^2 \cdot Re_{\mathrm{air}}^{-0.25} \tag{6}$$

where Reynolds number $Re_{\mathrm{air}} = V_{\mathrm{air}} \cdot a_{\mathrm{air}} / 2v_{\mathrm{air}}$, ρ_{air} is the air density, a_{air} is the width between two fins, β_{air} is the thermal expansion coefficient of the air, $\Delta T_{air} = T_{\mathrm{air2}} - T_{\mathrm{air1}}$ is the air temperature difference between the top and bottom of the radiator fin, V_{air} is the average air velocity, and v_{air} is the kinematic viscosity of the air.

According to the conservation of energy, the heat absorbed by the air is equal to the heat transferred to the oil from total loss P, so:

$$P = \rho_{\mathrm{air}} \cdot c_{\mathrm{air}} \cdot Q_{\mathrm{air}} \cdot \Delta T_{\mathrm{air}} \tag{7}$$

$$Q_{\mathrm{air}} = V_{\mathrm{air}} \cdot a_{\mathrm{air}} \cdot W \cdot N \tag{8}$$

where c_{air} is the specific heat capacity of air, Q_{air} is the air flow rate, W is the width of the radiator fin, and N is the number of fins.

3) HEAT TRANSFER BETWEEN OIL FLOW AND AIR FLOW

After the heated oil flow enters the channel of fins, the heat is transferred to the air through the radiator wall. The total heat transfer coefficient without considering radiation heat dissipation is:

$$\frac{1}{r} = \frac{1}{r_{\mathrm{oil}}} + \frac{1}{r_{\mathrm{wall}}} + \frac{1}{r_{air}} \tag{9}$$

where r_{oil} and r_{air} are the heat transfer coefficients of the oil flow side and the air side respectively, $r_{\mathrm{wall}} = \lambda_{\mathrm{wall}} / \delta$ is the heat transfer coefficient of the radiator wall, λ_{wall} is the thermal conductivity of the radiator fin, and δ is the thickness of the radiator fin. Since $1/r_{\mathrm{wall}}$ is very small and more than 90% of the heat is carried away by convection between the radiator fan and the air [23], [25], the heat transfer effect on the air side is only considered.

Considering the structural distribution between the radiators, the convective heat dissipation between the air and the radiators can be approximately treated as a vertical plate [27], and the heat transfer coefficient of the air can be calculated as:

$$r_{\mathrm{air}} = Nu_{\mathrm{air}} \cdot \lambda_{\mathrm{air}} / y_{\mathrm{ra}} \tag{10}$$

$$Nu_{\mathrm{air}}^{1/2} = 0.825 + \frac{0.387 \cdot (\mathrm{Pr}_{\mathrm{air}} \cdot Gr_{\mathrm{air}})^{1/6}}{\left[1 + \left(0.492/\mathrm{Pr}_{\mathrm{air}}\right)^{9/16}\right]^{8/27}} \tag{11}$$

and the terms Pr_{air} and Gr_{air} are defined as follows [28]:

$$Gr_{\mathrm{air}} = \frac{g \cdot \beta_{\mathrm{air}}}{v_{\mathrm{air}}^2}(T_{\mathrm{oil}} - T_{\mathrm{air}}) \cdot y_{\mathrm{ra}}^3 \tag{12}$$

$$Pr_{\mathrm{air}} = \frac{\rho_{\mathrm{air}} \cdot v_{\mathrm{air}} \cdot c_{\mathrm{air}}}{\lambda_{\mathrm{air}}} \tag{13}$$

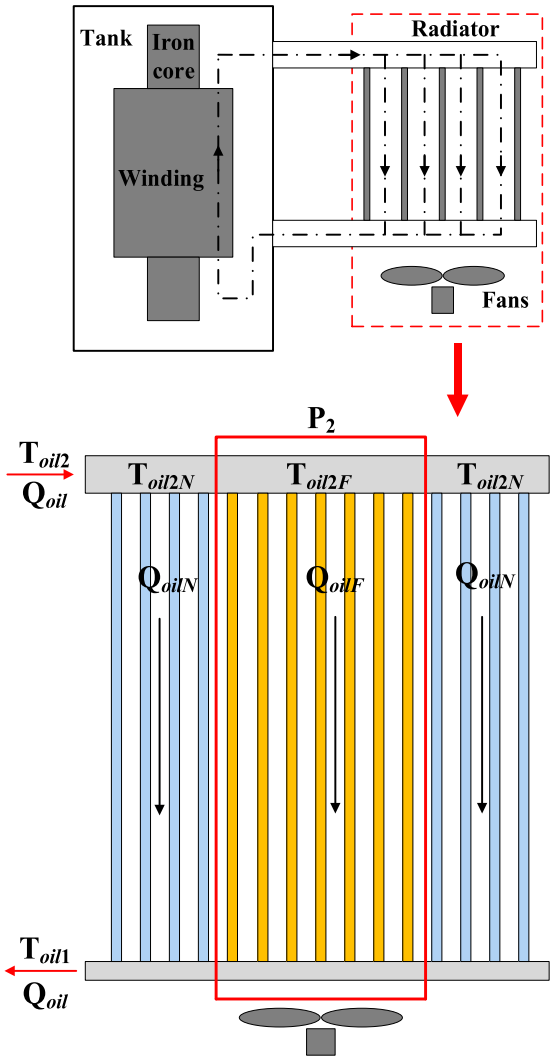

FIGURE 2. Flow and convection state of different parts in ONAF mode.

where λ_{air} is the thermal conductivity of air, T_{oil} and T_{air} are the oil flow temperature and the air temperature at same height respectively; Nu_{air}, Gr_{air} and Pr_{air} are the Nusselt number, Grashof number and Prandtl number of air, respectively. The temperature rise equations can be established according to the temperature distribution along the oil channel in fins:

$$\frac{d\left(T_{oil}-T_{air}\right)}{d\left[S/\left(T_{oil2}-T_{oil1}\right)\right]}=-h\left(T_{oil}-T_{air}\right) \tag{14}$$

$$h=r\cdot\left[\left(1/\rho cQ\right)_{oil}-\left(1/\rho cQ\right)_{air}\right] \tag{15}$$

$$T_{oil2}-T_{air2}=\left(T_{oil1}-T_{air1}\right)\cdot e^{-h\cdot y_{ra}} \tag{16}$$

B. HEAT TRANSFER FROM OIL TO AIR IN ONAF MODE

Considering that some of the heatsinks cannot be blown by the fan in air-cooling mode, the cooling effect is the result of the combined effect of natural and forced cooling.

In ONAF mode, the function of the fan is to make the natural convection to forced convection. Compared with ONAN mode, the conservation of momentum on the air side no longer holds. To set up the momentum expression on the air side, the wind speed from fans as the external input parameters should be involved in above modelling. So, the average Reynolds number and average Nusselt number have been changed as [29]:

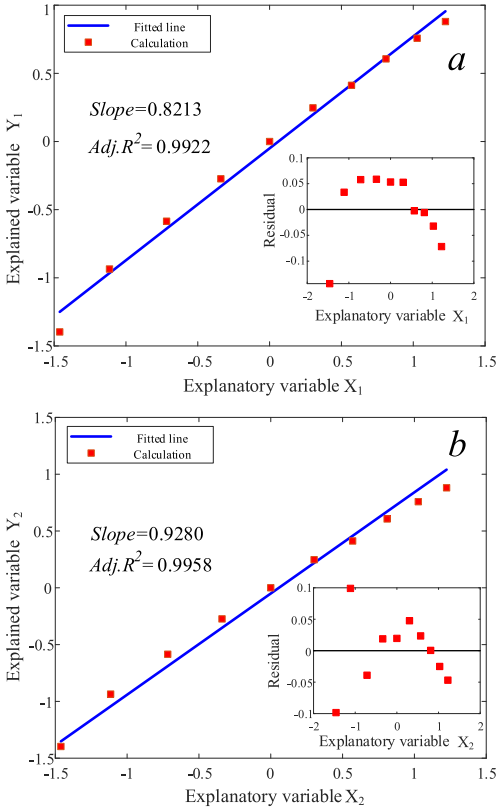

FIGURE 3. Comparison result graph of oil exponent. (a) in ONAN mode. (b) in ONAF mode.

$$Re_{airF}=V_{airF}\cdot y_{ra}/v_{air} \tag{17}$$

$$Nu_{airF}=\frac{0.6774\cdot\left(Re_{airF}\right)^{1/2}\cdot\left(Pr_{air}\right)^{1/3}}{\left[1+\left(0.0468/Pr_{air}\right)^{2/3}\right]^{1/4}} \tag{18}$$

where Pr_{airF} is the Prandtl number of forced air flow, V_{airF} is the average air velocity from fans.

For a radiator with N fins, the heat dissipation power of N_1 fins in ONAN mode is P_1, and that of N_2 fins in ONAF mode is P_2. The inlet oil and global oil flow in both modes should be the same value. The coupling schematic diagram is shown in Figure 3, so it is considered as:

$$P=P_1+P_2 \tag{19}$$

$$N=N_1+N_2 \tag{20}$$

$$T_{oil2}=T_{oil2N}=T_{oil2F} \tag{21}$$

$$Q_{oil}=Q_{oilN}=Q_{oilF} \tag{22}$$

where P is the total loss, Q_{oil} is whole oil flow through the radiator, while T_{oil2N}, Q_{oilN}, T_{oil2F} and Q_{oilF} are inlet

TABLE 1. Material properties used in modelling.

Symbol	Fitting function or value
$\rho_{oil}(T)$	889-0.671T kg/m^3
$c_{oil}(T)$	1973+4.01T J/(kg·K)
$v_{oil}(T)$	exp[$e^{24.74}$×(T+273)$^{-4.2}$-0.7]×10^{-6} m^2/s
β_{oil}	7.9×10^{-4} 1/K
ρ_{air}	1.1769 kg/m^3
c_{air}	1006.3 J/(kg·K)
λ_{air}	0.02624 W/(m·K)
v_{air}	1.8464×10^{-5} m^2/s
β_{air}	3.3×10^{-3} 1/K

TABLE 2. Transformer nameplate information for calculation.

Symbol	Transformer parameters	Value
P	Rated capacity	120 MVA
P_{rated}	Rated total loss	178 kW
R	Ratio of rated load loss to no-load loss	4.2

TABLE 3. Radiator design parameters.

Symbol	Radiator design parameters	Parameter values
y_{ra}	Radiator height	2600 mm
Δy	The height between the winding and the radiator	450 mm
W	Radiator width	520 mm
N	Number of panels	22
b_{oil}/a_{oil}	Ratio of length to width of rectangular oil channel	14.29
s_c	Oil flow channel area	3.25×10^{-4} m^2
d_c	Perimeter of oil flow channel	0.3045 m
a_{air}	Radiator spacing	50 mm
V_{air}	Wind speed at full power	3.37 m/s

oil temperature and oil flow through the fins under natural convection and forced convection, respectively.

IV. ANALYSIS OF OIL EXPONENT FOR ONAN AND ONAF COOLING MODE

A. CASE OBJECT

In this paper, physical parameters such as density, kinematic viscosity, and thermal conductivity of fluids involved in the calculation are shown in Table 1 below. An oil-immersed transformer with rated capacity of 120-MVA and rated voltage of 220-kV was chosen as the case object, which has been equipped with radiators (PC2600-22/520). Its specific parameters are shown in Table 2. Table 3 shows the design parameters of the radiator.

B. SOLVING THE OIL EXPONENTS

Through the above subsections, TOT rise under different load can be obtained under ONAN cooling mode as well as ONAF cooling mode. The different trends of TOT rise reflect the differences between ONAN and ONAF.

Oil exponent is a parameter that links the trends of TOT rise and the dynamic thermal modelling of oil-immersed transformer. Naturally, oil exponent is a rational eigenvalue to reflect the condition of fans. In order to use linear regression to fit the oil exponent, we take the natural logarithm according to the definition as:

$$\ln\left(\frac{\Delta T_{oil}}{\Delta T_{oil,rated}}\right) = n \cdot \ln\left(\frac{I_{pu}^2 R + 1}{R + 1}\right) \tag{23}$$

where ΔT_{oil} is the TOT rise, $\Delta T_{oil,rated}$ is the rated TOT rise, I_{pu} is the load current per unit, and n represents the oil exponent. Let the variable $Y = \ln(\Delta T_{oil}/\Delta T_{oil,rated})$, and let the variable $X = \ln\left(I_{pu}^2 R + 1 \Big/ R + 1\right)$. As shown in Figure 3, group (X_1, Y_1) and group (X_2, Y_2) represent the data of ONAN and ONAF, respectively.

According to the comparison results of oil exponent, the oil exponent of ONAN cooling mode and ONAF cooling mode are 0.8213 and 0.9280, respectively, which indicates that the significant difference between the two cooling modes by oil exponent. The above results prove once again that oil exponent can be used as a characteristic criterion to reflect the airflow volume from the fan, and providing a theoretical basis for the next online monitoring to the abnormal state of the fan.

V. PSO-BASED OIL EXPONENT TRACKING

A. PSO ALGORITHM FOR PARAMETER TRACKING

PSO uses particle search for the optimal solution from imitating the behavior of bird foraging. Its basic idea is to solve the target optimal value through collaboration and information sharing among individuals in the group, which has the advantages of fewer adjustable parameters, fast convergence, and high precision.

PSO algorithm is initialized by a bunch of random particles, each of which has its own two properties: velocity V and position X, where velocity indicates how fast and how slow it is moving, and position indicates the direction it is moving.

Each particle separately searches for the optimal solution in the given space, which is remarked as the current individual optimal value P_{best}. Then, by comparing with the individual extremum of other particles in the whole particle swarm, the current global optimal solution set G_{best} could be found. Further, all particles update their speed and position according to their individual extremum and the current global optimal set. The final optimal solution satisfying the termination condition will be finally found through iteration. The iterative formula for velocity and position of no. $\boldsymbol{i}$ particle is as follows:

$$\begin{aligned} V_i^{t+1} &= \omega V_i^t + c_1 \cdot rand(0,1) \cdot \left(P_i - X_i^t\right) \\ &\quad + c_2 \cdot rand(0,1) \cdot \left(G_i - X_i^t\right) \end{aligned} \tag{24}$$

$$X_i^{t+1} = X_i^t + V_i^{t+1} \tag{25}$$

where ω is the inertia weight between 0-1, c_1 is the individual learning factor and c_2 is the social learning factor of the particle.

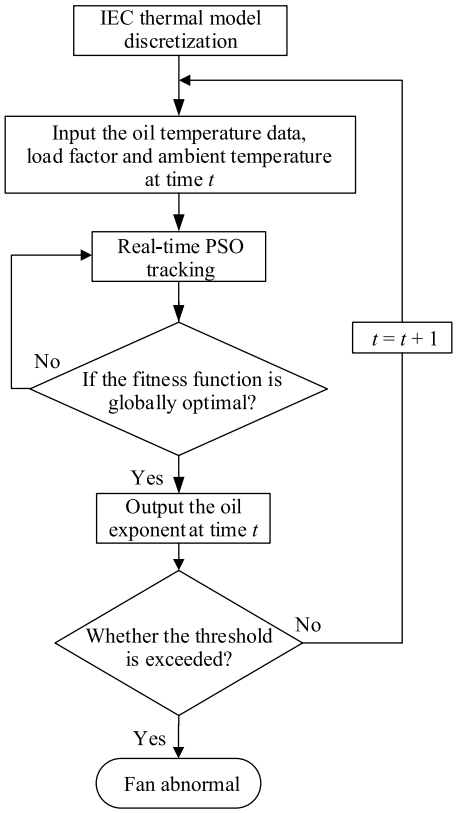

FIGURE 4. Oil exponent tracking flow chart.

Regarding the parameter setting in PSO iteration, based on equations (24) and (25), the parameters are set as follows: the initial number of populations is 100, the individual learning factor c_1 and the social learning factor c_2 of the particles are both taken as 2, the inertia weight ω is taken as 0.8 and the maximum number of iterations is 300, the upper limit of iteration is 1 and the lower limit is 0.8.

B. OIL EXPONENT TRACKING

According to the obtained oil exponents, PSO was used to monitor the variation of oil exponent, as shown in Figure 4. According to the improved IEC 60076-7 top-oil thermal model by authors in [18], the TOT is calculated as follows:

$$\left(\frac{1+RI_{pu}^2}{1+R}\right)^n \Delta T_{oil,rated} = \tau_{oil}\frac{dT_{oil}}{dt} + (T_{oil} - T_{amb}) \quad (26)$$

where n is the oil exponent, and θ_{amb} is the ambient temperature. From then on, T_{oil} refers specifically to the TOT. τ_{oil} is the oil time constant, which has been calibrated as:

$$\frac{\tau_{oil}}{\tau_{oil,rated}} = \frac{\left(\frac{1+RI_{pu}^2}{1+R}\right)^n - \left(\frac{T_{oil}-T_{amb}}{\Delta T_{oil,rated}}\right)}{\left(\frac{1+RI_{pu}^2}{1+R}\right) - \left(\frac{T_{oil}-T_{amb}}{\Delta T_{oil,rated}}\right)^{\frac{1}{n}}} \quad (27)$$

where $\tau_{oil,rated}$ is the rated oil time constant. From (27), it is noted that τ_{oil} has been calibrated as a changing parameter. Since (26) was introduced for PSO, a discrete-time form of (26) with Euler approximation can be derived as [16]:

$$T_{oil}(k) = \frac{\tau_{oil}}{\tau_{oil}+\Delta t}T_{oil}(k-1) + \frac{\Delta t}{\tau_{oil}+\Delta t}T_{amb}(k) + \frac{\Delta t}{\tau_{oil}+\Delta t}\left[\frac{1+RI_{pu}^2(k)}{1+R}\right]^n \Delta T_{oil,rated} \quad (28)$$

where the varying oil time constant τ_{oil} should be substituted as (27), Δt is the sampling interval and takes as 1 minute. The top oil temperature T_{oil}, ambient temperature T_{amb}, load factor I_{pu}, oil time constant τ_{oil}, rated temperature rise $\Delta T_{oil,rated}$ and R at each moment are involved in the iterative solution as known input variables, where rated temperature rise and R are known constant values for the same oil-immersed transformer and R is the ratio of rated load loss to no-load loss. Thus, in equation (28), only the oil exponent n remains as an unknown variable. It should be noted that (27) also needs to be discretised as (29), where the term $T_{oil}(k-1) - T_{amb}(k-1)$ is from last iteration while the load current per unit $I_{pu}(k)$ is for current iteration, namely as

$$\frac{\tau_{oil}}{\tau_{oil,rated}} = \frac{\left[\frac{1+RI_{pu}^2(k)}{1+R}\right]^n - \left[\frac{T_{oil}(k-1)-T_{amb}(k-1)}{\Delta T_{oil,rated}}\right]}{\left[\frac{1+RI_{pu}^2(k)}{1+R}\right] - \left[\frac{T_{oil}(k-1)-T_{amb}(k-1)}{\Delta T_{oil,rated}}\right]^{\frac{1}{n}}} \quad (29)$$

VI. VERIFICATIONS FOR DETECTING METHOD BASED ON OIL EXPONENT TRACKING: CASE STUDY

In order to verify the effectiveness of the above method, two cases in different scenarios were presented. It should be noted that the real potential malfunction is difficult to produce in field, while we can use two common scenarios to verify it indirectly. And from the following cases, we can know the relationship between fans' condition (including malfunction state) and varying oil exponent.

A. CASE 1: ALL FANS SHUTTING DOWN

According to the TOT data, load current per unit, and ambient temperature of the oil-immersed transformer within 15 days, the transformer changed from ONAF cooling mode to ONAN cooling mode at 8 am of the 10th day. A PSO algorithm was used to identify the oil exponent of the TOT data, and the results were shown in Figure 5.

From October 31 to November 8, when the transformer was working in the ONAF cooling mode, the predicted oil exponent value was stable between 0.9-0.95, which fluctuated within an acceptable range. After the fan shut down at 8 a.m. on November 9, the transformer switched to ONAN cooling mode. Due to the lag of transformer oil temperature change, the oil exponent did not drop immediately after the fan turning off, and gradually decreased and finally stabilized between 0.8-0.85, which was consistent with the expected results from the above analysis. It can be seen from the variation of local

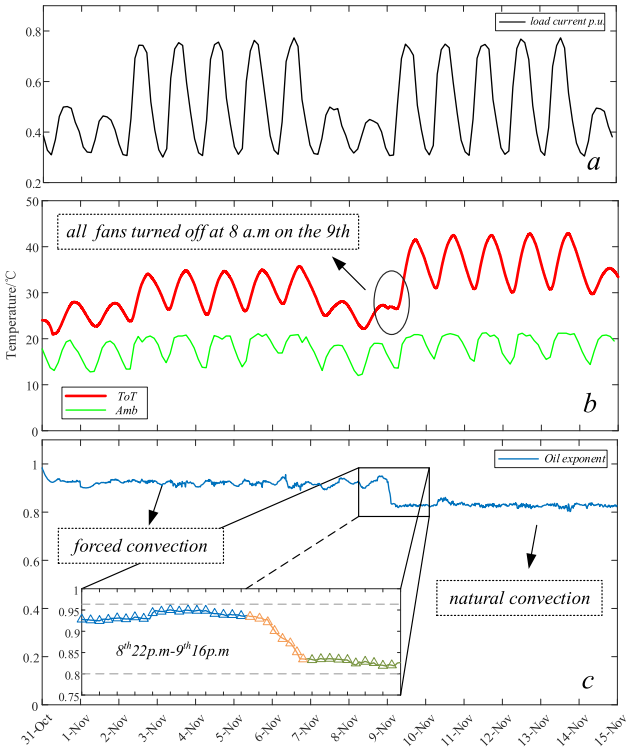

FIGURE 5. Case in all fans shutting down scenario. (a) load profile. (b) TOT, ambient temperature and fans' operating condition. (c) tracking oil exponent.

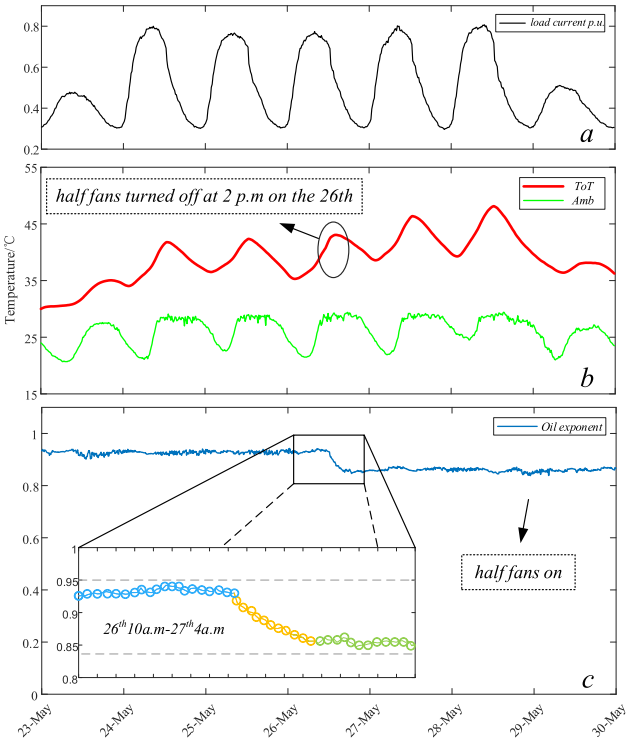

FIGURE 6. Case in half fans shutting down scenario. (a) load profile. (b) TOT, ambient temperature and fans' operating condition. (c) tracking oil exponent.

oil exponent before and after the failure that the oil exponent can sensitively identify the inner change implied by the TOT and reflect the abnormal state by means of the airflow volume during online monitoring. So, the TOT monitoring not only achieved the goal of controlling TOT rise but also indirectly detect the abnormal state of fans without more sensors.

B. CASE 2: HALF FANS SHUTTING DOWN

To investigate the intermediate between all shutting down and all turning on, the TOT data containing half fans shutting down was chosen for verification. As shown in Figure 5, half fans shut down on 2 p.m. at May 26.

As shown in Figure 6, before fans shutting down, the predicted oil exponent also was stable between 0.9-0.95. After half fans shut down, the transformer turned to an incomplete ONAF cooling state. The oil exponent gradually dropped into the range between 0.84-0.86.

In summary, two operating conditions show the change in top oil temperature and the consequent effect on the oil exponent when the transformer cooling mode is switched between full-on, half-on and full-off fan operation states, respectively. The results of the study are all in line with the modeling calculation trends and consistent with the expected values. If Figure 5 is a verification of the logical accuracy of this research method, Figure 6 can be seen as a further example verification of this method, further illustrating the accuracy and effectiveness of the oil exponent as a detection of early fan failure.

In addition, the transformer overheating defects caused by increased load losses, oil temperature fluctuations caused by normal changes in load, in the analysis of the oil exponent as well as real-time identification methods, are considered in the transformer load input, operating losses, rated temperature rise and external environment and other factors, the identification results show that its effect on the overall top oil temperature rise is not enough to cause a sustained and significant change in the oil exponent, further This further confirms the validity and accuracy of the oil exponent as a characteristic parameter of the fan operating condition under such circumstances. Therefore, when the oil exponent changes continuously beyond the threshold value or does not match the expected value, it indicates a change in the fan-side operating status and the occurrence of early faults at this time, which an alarm should be issued and checked in time.

We concern that further detailed classification and study of the oil exponent is the key to achieving online intelligent monitoring of the operating condition of oil-immersed transformer cooling fans. Due to the limited data collected and experimental conditions, we were not able to delineate in detail the oil exponent reference values for all operating conditions in this manuscript, which is the focus of our upcoming work and research.

VII. CONCLUSION

In order to realize the real-time detection for fans' malfunction, a method exerting the existing TOT monitoring was presented.

1) The oil exponent under ONAN cooling mode and ONAF cooling mode are 0.8213 and 0.9280, respectively, indicating that the oil exponent has a certain significance in distinguishing the two cooling modes. Furthermore, the range between two endpoint values reflects the air flow change.

2) Taking oil exponent as eigenvalue, a method monitoring air flow was proposed, where the change of oil exponent reflects the different condition of fans. A PSO algorithm was used to track the oil exponent. The effectiveness of this method is demonstrated by two cases.

The above findings and method provide a new way for early fault detecting of fans. It should be mentioned that this method is expected to be valid for other practical cases. The influence of transformer internal overheating defects on the change of oil exponent reference value, the relationship between multiple operating conditions of transformers and oil exponent reference value, and the correspondence between quantifying the oil exponent reference value and fan operating faults will be the focus of our future research.

REFERENCES

[1] D. Wang, L. Zhou, Z.-X. Yang, Y. Cui, L. Wang, J. Jiang, and L. Guo, "A new testing method for the dielectric response of oil-immersed transformer," *IEEE Trans. Ind. Electron.*, vol. 67, no. 12, pp. 10833–10843, Dec. 2020.

[2] L. Zhou, J. Cai, J. Hu, G. Lang, L. Guo, and L. Wei, "A correction-iteration method for partial discharge localization in transformer based on acoustic measurement," *IEEE Trans. Power Del.*, vol. 36, no. 3, pp. 1571–1581, Jun. 2021.

[3] Y. Gao, B. Patel, Q. Liu, Z. Wang, and G. Bryson, "Methodology to assess distribution transformer thermal capacity for uptake of low carbon technologies," *IET Gener., Transmiss. Distrib.*, vol. 11, no. 7, pp. 1645–1651, May 2017.

[4] X. Jin, E. W. M. Ma, L. L. Cheng, and M. Pecht, "Health monitoring of cooling fans based on Mahalanobis distance with mRMR feature selection," *IEEE Trans. Instrum. Meas.*, vol. 61, no. 8, pp. 2222–2229, Aug. 2012.

[5] S. Anishek, R. Sony, J. J. Kumar, and P. M. Kamath, "Performance analysis and optimisation of an oil natural air natural power transformer radiator," *Proc. Technol.*, vol. 24, pp. 428–435, Jan. 2016.

[6] U. SanAndres, G. Almandoz, J. Poza, and G. Ugalde, "Design of cooling systems using computational fluid dynamics and analytical thermal models," *IEEE Trans. Ind. Electron.*, vol. 61, no. 8, pp. 4383–4391, Aug. 2014.

[7] S. C. Zhao, X. Zhang, Q. Liu, M. Wilkinson, M. Nergo, and M. Daghrah, "Effect of thermal conduction on transformer radiator CFD modelling," in *Proc. 8th Int. Conf. Condition Monitor. Diagnosis (CMD)*, Oct. 2020, pp. 242–245.

[8] S. Dasgupta, A. Nandwana, and K. Ravikumar, "Flow channelization method to enhance transformer radiator cooling capacity," *J. Thermal Sci. Eng. Appl.*, vol. 10, no. 6, Dec. 2018, Art. no. 064501.

[9] W. Van Der Veken, S. B. Paramane, R. Mertens, V. Chandak, and J. Codde, "Increased efficiency of thermal calculations via the development of a full thermohydraulic radiator model," *IEEE Trans. Power Del.*, vol. 31, no. 4, pp. 1473–1481, Aug. 2016.

[10] S. B. Paramane, K. Joshi, W. Van der Veken, and A. Sharma, "CFD study on thermal performance of radiators in a power transformer: Effect of blowing direction and offset of fans," *IEEE Trans. Power Del.*, vol. 29, no. 6, pp. 2596–2604, Dec. 2014.

[11] Y. J. Kim, M. Jeong, Y. G. Park, and M. Y. Ha, "A numerical study of the effect of a hybrid cooling system on the cooling performance of a large power transformer," *Appl. Thermal Eng.*, vol. 136, pp. 275–286, May 2018.

[12] J. Wu, P. Guo, Y. Cheng, H. Zhu, X.-B. Wang, and X. Shao, "Ensemble generalized multiclass support-vector-machine-based health evaluation of complex degradation systems," *IEEE/ASME Trans. Mechatronics*, vol. 25, no. 5, pp. 2230–2240, Oct. 2020.

[13] X.-B. Wang, Z.-X. Yang, and X.-A. Yan, "Novel particle swarm optimization-based variational mode decomposition method for the fault diagnosis of complex rotating machinery," *IEEE/ASME Trans. Mechatronics*, vol. 23, no. 1, pp. 68–79, Feb. 2018.

[14] X. Gong and W. Qiao, "Current-based mechanical fault detection for direct-drive wind turbines via synchronous sampling and impulse detection," *IEEE Trans. Ind. Electron.*, vol. 62, no. 3, pp. 1693–1702, Mar. 2015.

[15] *Power Transformers—Part 7: Loading Guide for Oil-Immersed Power Transformers*, Standard IEC 60076-7, 2005.

[16] B. C. Lesieutre, W. H. Hagman, and J. L. Kirtley, "An improved transformer top oil temperature model for use in an on-line monitoring and diagnostic system," *IEEE Trans. Power Del.*, vol. 12, no. 1, pp. 249–256, Jan. 1997.

[17] L. Jauregui-Rivera and D. J. Tylavsky, "Acceptability of four transformer top-oil thermal models—Part II: Comparing metrics," *IEEE Trans. Power Del.*, vol. 23, no. 2, pp. 866–872, Apr. 2008.

[18] L. Wang, X. Zhang, R. Villarroel, Q. Liu, Z. Wang, and L. Zhou, "Top-oil temperature modelling by calibrating oil time constant for an oil natural air natural distribution transformer," *IET Gener., Transmiss. Distrib.*, vol. 14, no. 20, pp. 4452–4458, Oct. 2020.

[19] Y. Cui, H. Ma, T. Saha, C. Ekanayake, and D. Martin, "Moisture-dependent thermal modelling of power transformer," *IEEE Trans. Power Del.*, vol. 31, no. 5, pp. 2140–2150, Oct. 2016.

[20] D. Susa and H. Nordman, "IEC 60076-7 loading guide thermal model constants estimation," *Int. Trans. Electr. Energy Syst.*, vol. 23, no. 7, pp. 946–960, Oct. 2013.

[21] D. Peterchuck and A. Pahwa, "Sensitivity of transformer's hottest-spot and equivalent aging to selected parameters," *IEEE Trans. Power Del.*, vol. 17, no. 4, pp. 996–1001, Oct. 2002.

[22] L. Wang, L. Zhou, H. Tang, D. Wang, and Y. Cui, "Numerical and experimental validation of variation of power transformers' thermal time constants with load factor," *Appl. Therm. Eng.*, vol. 126, pp. 939–948, Nov. 2017.

[23] L. Zhou, L. Wang, H. Tang, J. Wang, L. Guo, and Y. Cui, "Oil exponent thermal modelling for traction transformer under multiple overloads," *IET Gener., Transmiss. Distrib.*, vol. 12, no. 22, pp. 5982–5989, Dec. 2018.

[24] K. Karsai, D. Kerenyi, and L. Kiss, *Large Power Transformers*. New York, NY, USA: Elsevier, 1987.

[25] L. Wang, L. Zhou, S. Yuan, J. Wang, H. Tang, D. Wang, and L. Guo, "Improved dynamic thermal model with pre-physical modelling for transformers in ONAN cooling mode," *IEEE Trans. Power Del.*, vol. 34, no. 4, pp. 1442–1450, Aug. 2019.

[26] R. B. Dean, "Reynolds number dependence of skin friction and other bulk flow variables in two-dimensional rectangular duct flow," *J. Fluids Eng.*, vol. 100, no. 2, pp. 215–223, Jun. 1978.

[27] S. W. Churchill and H. H. S. Chu, "Correlating equations for laminar and turbulent free convection from a vertical plate," *Int. J. Heat Mass Transf.*, vol. 18, no. 11, pp. 1323–1329, Nov. 1975.

[28] J. R. Welty, G. L. Rorrer, and D. G. Foster, *Fundamentals of Momentum, Heat and Mass Transfer*, 6th ed. New York, NY, USA: Wiley, 2013.

[29] S. W. Churchill, "A comprehensive correlating equation for forced convection from flat plates," *AIChE J.*, vol. 22, no. 2, pp. 264–268, Mar. 1976.

LUJIA WANG (Member, IEEE) received the B.Sc. and Ph.D. degrees in electrical engineering from Southwest Jiaotong University, Chengdu, China, in 2015 and 2020, respectively. He was a joint Ph.D. Student with the School of Electrical and Electronic Engineering, The University of Manchester, Manchester, U.K. Since 2020, he has been a Lecturer with the School of Electrical and Power Engineering, China University of Mining and Technology, Xuzhou, China. His current research interests include thermal modeling and fault diagnosis for electrical equipment.

WANWAN ZUO received the B.Sc. degree in electrical engineering from Wuhan University of Technology, Wuhan, China, in 2019. She is currently pursuing the M.Sc. degree in electrical engineering with the School of Electrical and Power Engineering, China University of Mining and Technology, Xuzhou, China. Her main research interest includes the condition monitoring for cooling systems.

ZHI-XIN YANG (Member, IEEE) received the B.Eng. degree in mechanical engineering from Huazhong University of Science and Technology, China, in 1992, and the Ph.D. degree in industrial engineering and engineering management from The Hong Kong University of Science and Technology, in 2000. He is currently an Associate Professor with the State Key Laboratory of Internet of Things for Smart City, Department of Electromechanical Engineering, University of Macau, Macau, China. His research interests include the Internet of Things (IoTs)-based urban safety monitoring and disaster prevention, prognostic health monitoring (PHM) and fault diagnosis for engineering systems, and computer vision (CV) and artificial intelligence-based robotic control.

JIANWEN ZHANG received the B.Eng. and M.Sc. degrees from Xi'an Jiaotong University, Xi'an, China, in 1990 and 1998, respectively, and the Ph.D. degree from China University of Mining and Technology, Xuzhou, China, in 2003. He is currently a Professor with the School of Electrical and Power Engineering, China University of Mining and Technology. His research interests include high-voltage technology, condition monitoring, and fault diagnosis technology for electrical equipment.

ZHENLU CAI received the B.Sc. degree in electrical engineering from Xuzhou University of Technology, Xuzhou, China, in 2020. He is currently pursuing the M.Sc. degree in electrical engineering with the School of Electrical and Power Engineering, China University of Mining and Technology, Xuzhou. His main research interest includes the condition monitoring for power transformer.